

First Observation of $\overline{B}^0 \rightarrow D^{*0}\pi^+\pi^+\pi^-\pi^-$ Decays

Abstract

We report on the observation of $\overline{B}^0 \rightarrow D^{*0}\pi^+\pi^+\pi^-\pi^-$ decays. The branching ratio is $(0.30 \pm 0.07 \pm 0.06)\%$. Interest in this particular mode was sparked by Ligeti, Luke and Wise who propose it as a way to check the validity of factorization tests in $\overline{B}^0 \rightarrow D^{*+}\pi^+\pi^-\pi^-\pi^0$ decays.

1 Introduction

In previous work we found a large branching fraction of $(1.72 \pm 0.14 \pm 0.24)\%$ for the decay $\overline{B}^0 \rightarrow D^{*+}\pi^+\pi^-\pi^-\pi^0$ [1]. This reaction can proceed via several possible tree level processes. The simplest diagram, shown in Fig. 1(a), has the four-pions emitted from the virtual W^- . Assuming that this is indeed the dominant process, Ligeti, Luke and Wise (LLW) [2] have compared the invariant mass spectrum from our data with $\tau^- \rightarrow \pi^+\pi^-\pi^-\pi^0$ data (also from CLEO) [3]. Using a model based on factorization [4] they show that the data agree up to four- π^- invariant mass squared of 2.8 GeV^2 , within an error of about 15%.

However, the agreement may be fortuitous, rather than a success of factorization, if other diagrams are present. For example another possible diagram is shown in Fig. 1(b), where the D^{*+} and the π^0 are produced at the lower vertex and the virtual W^- manifests as $\pi^+\pi^-\pi^-$. This process was searched for in the original publication. Definite evidence was lacking but a stringent upper limit could not be set.

Here we search for the process $\overline{B}^0 \rightarrow D^{*0}\pi^+\pi^+\pi^-\pi^-$ as suggested by LLW. This can be produced by the diagram in Fig. 1(b), where the D^{*0} combines with one of the π^+ 's to form a low-mass system. It could also be produced by the color-suppressed process shown in Fig. 1(c).

In this paper we indeed show that the process $\overline{B}^0 \rightarrow D^{*0}\pi^+\pi^+\pi^-\pi^-$ has a significant branching ratio and try to ascertain the dominant production mechanism.

The data sample consists of 9.0 fb^{-1} of integrated luminosity taken with the CLEO II and II.V detectors [5] using the CESR e^+e^- storage ring on the peak of the $\Upsilon(4S)$ resonance and 4.4 fb^{-1} in the continuum at 60 MeV less center-of-mass energy. The sample contains 19.4 million B mesons.

2 Selection Criteria

Hadronic events are selected by requiring a minimum of five charged tracks, total visible energy greater than 15% of the center-of-mass energy, and a charged track vertex consistent with the nominal interaction point. To reject continuum we require that the Fox-Wolfram moment R_2 be less than 0.3 [6].

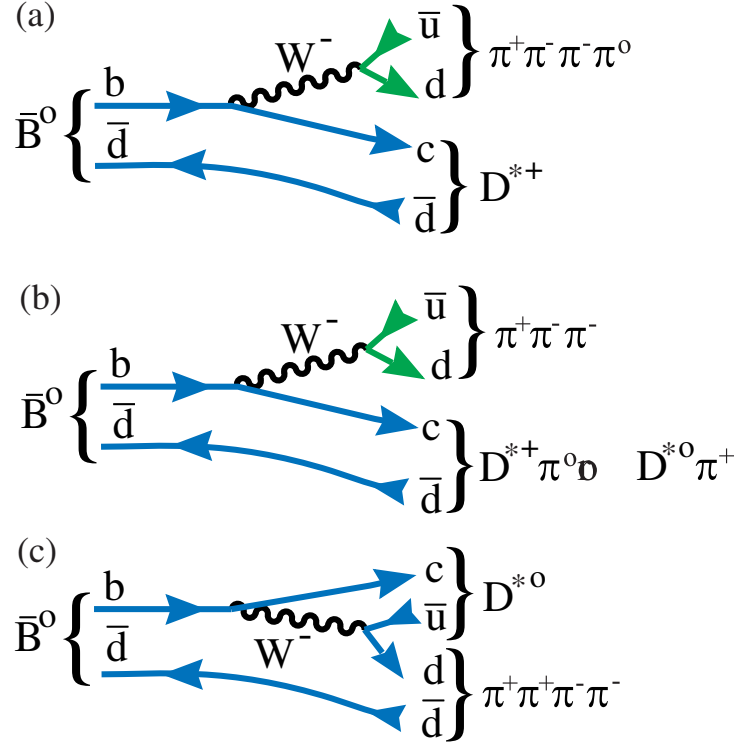


Figure 1: Diagrams for $\bar{B} \rightarrow D^* \pi \pi \pi \pi$ decays. (a) Charged current tree level diagram for $D^{*+}(4\pi)^-$. (b) Charged current tree level diagram for $(D^{*+}\pi^0)\pi^+\pi^-\pi^-$ or $(D^{*0}\pi^+)\pi^+\pi^-\pi^-$. The $D^*\pi$ system can form a D^{**} resonance. (c) Color suppressed diagram for $D^{*0}(4\pi)^0$.

Track candidates are required to pass through a common spatial point defined by the origin of all tracks. Tracks with momentum below 900 MeV/c are required to have an ionization loss in the drift chamber within 3σ of that expected for their assigned mass. Photon candidates are required to be in the “good barrel region,” within 45° of the plane perpendicular to the beam line that passes through the interaction point, and have an energy distribution in the CsI calorimeter consistent with that of an electromagnetic shower. To select π^0 's, we require that the diphoton invariant mass be between -3.0 to $+2.5\sigma$ of the π^0 mass, where σ varies with momentum and has an average value of approximately 5.5 MeV. The two-photon candidates are then kinematically fit by constraining their invariant mass be equal to the nominal π^0 mass.

We select D^0 candidates in the $K^-\pi^+$ decay mode. We require that the invariant mass of the D^0 candidates lie within $\pm 2.5\sigma$ of the known D^0 mass. The D^0 width varies with the D^0 momentum, p , as $p \times 0.93 \times 10^{-3} + 6.0$ (units of MeV).

We use the analogous requirement on the $D^{*0}-D^0$ mass difference. In this case the mass difference resolution is 0.90 MeV [8].

3 Observation of $\overline{B}^0 \rightarrow D^{*0} \pi^+ \pi^+ \pi^- \pi^-$ Decays

We start by looking for the $D^{*0}(4\pi)^0$ final state.* The D^{*0} candidates are pooled with all combinations of $\pi^+ \pi^+ \pi^- \pi^-$ mesons.

Next, we calculate the difference between the beam energy, E_{beam} , and the measured energy of the five particles, ΔE . The “beam constrained” invariant mass of the B candidates, M_B , is computed from the formula

$$M_B^2 = E_{beam}^2 - \left(\sum_i \vec{p}_i \right)^2 \quad . \quad (1)$$

To further reduce backgrounds we define

$$\chi_b^2 = \left(\frac{\Delta M_{D^*}}{\sigma(\Delta M_{D^*})} \right)^2 + \left(\frac{\Delta M_D}{\sigma(\Delta M_D)} \right)^2 + \left(\frac{\Delta M_{\pi^0}}{\sigma(\Delta M_{\pi^0})} \right)^2 \quad , \quad (2)$$

where ΔM_{D^*} is the computed $D^* - D^0$ mass difference minus the nominal value, ΔM_D is the invariant candidate D^0 mass minus the known D^0 mass and ΔM_{π^0} is the measured $\gamma\gamma$ invariant mass minus the known π^0 mass. The σ 's are the measurement errors. We select candidate events in each mode requiring that $\chi_b^2 < 5$.

4 Branching Fraction and $(4\pi)^0$ Mass Spectrum

We show the candidate B mass distribution, M_B , for ΔE in the side-bands from -6.0 to -4.0σ and 4.0 to 6.0σ on Fig. 2(a). The ΔE resolution is 14 MeV (σ). The sidebands give a good representation of the background in the signal region. We fit this distribution with a shape given as

$$back(r) = p_1 r \sqrt{1 - r^2} e^{-p_2(1-r^2)} \quad , \quad (3)$$

where $r = M_B/5.2895$, and the p_i are parameters given by the fit.

We next view the M_B distribution for events having ΔE within 2σ around zero in Fig. 2(b). This distribution is fit with a Gaussian signal function of width 2.7 MeV and the background function found above whose normalization is allowed to vary. The Gaussian signal width is found from Monte Carlo simulation. The largest and dominant component results from the energy spread of the beam. We find a total of 64 ± 16 signal events indicating that this decay mode is indeed different from zero.

We have investigated two mode-specific backgrounds that could, in principle, induce fake signals. These include the final states $D^{*+} \pi^+ \pi^- \pi^- \pi^0$ where we miss the slow π^+ from the D^{*+} decay and the π^0 and D^0 happen to satisfy the D^{*0} requirement, and $D^0 \pi^+ \pi^+ \pi^- \pi^- \pi^0$, where the D^0 and the π^0 happen to satisfy the D^{*0} requirement. We find that the efficiencies for each of these modes to contribute are small. The first final state was measured as having a branching ratio of 1.72% [1]. It would contribute 0.42 ± 0.47 events. The second final state never been measured. It would contribute 1.59 ± 0.53 events per 1% branching ratio. Considering that we observe 64 ± 16 signal events, these contributions are small.

*In this paper $(4\pi)^0$ will always denote the specific combination $\pi^+ \pi^+ \pi^- \pi^-$.

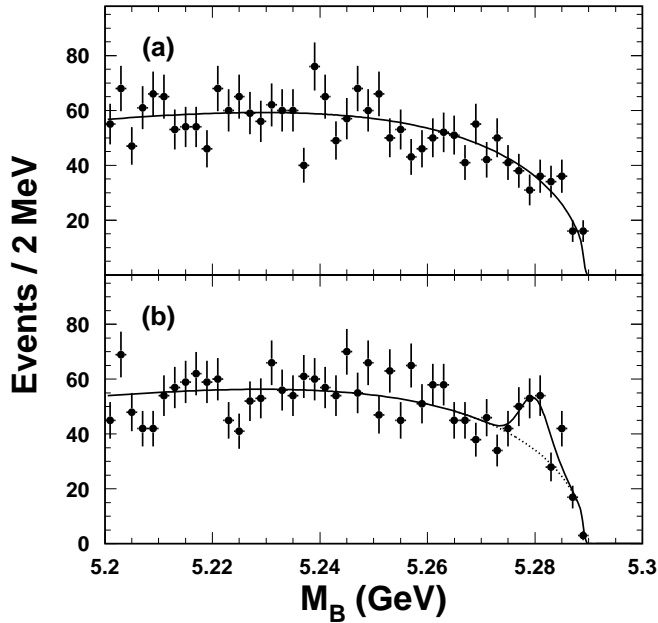


Figure 2: The B candidate mass spectra for the final state $D^{*o}\pi^+\pi^+\pi^-\pi^-$, (a) ΔE sidebands, (b) for ΔE consistent with zero. The curve in (a) shows a fit to the background distribution described in the text, while in (b) shapes from (a) is used with the normalization allowed to float and a signal Gaussian of width 2.7 MeV is added.

In order to find the branching ratio we use the Monte Carlo generated efficiency, shown in Fig. 3 as a function of $(4\pi)^o$ mass.

Since the efficiency varies with mass we need to determine the $(4\pi)^o$ mass spectrum in order to determine the branching ratio. To rid ourselves of the problem of the background shape, we fit the B candidate mass spectrum in 100 MeV bins of $(4\pi)^o$ mass. The resulting $(4\pi)^o$ mass spectrum is shown in Fig. 4.

We find

$$\mathcal{B}(\bar{B}^o \rightarrow D^{*o}\pi^+\pi^+\pi^-\pi^-) = (0.30 \pm 0.07 \pm 0.06)\% \quad . \quad (4)$$

The systematic error arises mainly from our lack of knowledge about the tracking and π^o efficiencies. We assign errors of $\pm 2.2\%$ on the efficiency of each charged track, and $\pm 5.4\%$ for the π^o . The error due to the background shape is evaluated in three ways. First of all, we change the background shape by varying the fitted parameters by 1σ . This results in a change of $\pm 9.3\%$. Secondly, we allow the shape, p_2 , to vary (the normalization, p_1 , was already allowed to vary). This results in 11% decrease in the number of events. Finally, we choose a different background function

$$back'(r) = p_1 r \sqrt{1 - r^2} (1 + p_2 r + p_3 r^2 + p_4 r^3) \quad , \quad (5)$$

and repeat the fitting procedure. This results in a 9.3% increase in the number of events. Taking a conservative estimate of the systematic error due to the background shape we arrive

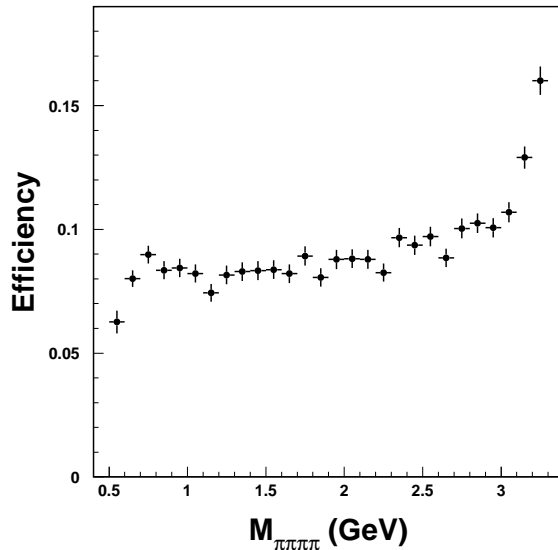


Figure 3: The efficiency for the final state $D^{*o}\pi^+\pi^-\pi^-\pi^-$.

at $\pm 11\%$. We use the current particle data group values for the relevant D^{*o} and D^o branching ratios of $(61.9 \pm 2.9)\%$ ($D^{*o} \rightarrow \pi^o D^o$) and $(3.83 \pm 0.09)\%$ ($D^o \rightarrow K^-\pi^+$), respectively [7]. The relative errors, 4.7% for the D^{*o} branching ratio and 2.3% for the D^o are added in quadrature to the background shape error, the π^o detection efficiency uncertainty and the tracking error. The total tracking error is found by adding the error in the charged particle track finding efficiency linearly for the 6 “fast” charged tracks and then in quadrature with the slow pion from the D^{*o} decay. The total positive systematic error is 19%. We also allow for cross-feed backgrounds amounting to 4 events giving a total negative systematic error of 20%.

5 Properties of the Final State

In Fig. 5(a) we show the $D^{*o}\pi^+$ invariant mass spectrum, obtained by fitting the number of \overline{B}^o events as a function of $D^{*o}\pi^+$ mass. (There are two combinations per event.) We also show for comparison the $D^{*o}\pi^-$ mass spectrum, where no structure is expected. We see evidence for an excess of events in the region of the $D^{**+}(2420)$ and $D^{**+}(2460)$. There are four D^{**} mesons. Two have relatively narrow widths and decay into $D^*\pi$, whereas two are wide, with only one decaying into $D^*\pi$ [9]. It is difficult to quantitatively evaluate the fraction of total D^{**+} production in our data. Selecting on the narrow states between 2.3 and 2.6 GeV, we find that $\sim 70\%$ of signal has one mass combination in this region.

In Fig. 6 we show the $\pi^+\pi^-\pi^-$ mass spectrum when the $D^{*o}\pi^+$ mass is required to be between 2.3 and 2.6 GeV. Here we fit the B yield as a function of $\pi^+\pi^-\pi^-$ mass. There is no clear feature present.

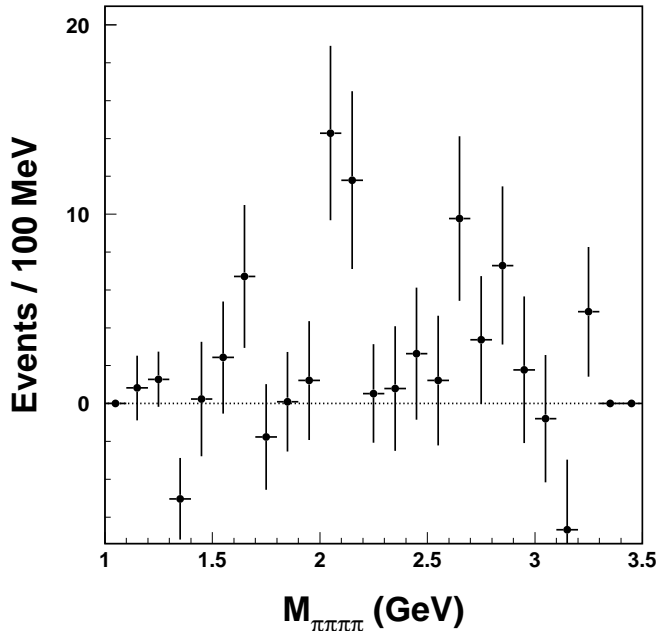


Figure 4: The invariant mass spectra of $\pi^+\pi^+\pi^-\pi^-$ for the final state $D^{*o}\pi^+\pi^+\pi^-\pi^-$, found by fitting the B yield in bins of 4π mass.

Let us now see how the presence of this final state affects the LLW prediction. In Fig. 7 we show the CLEO data [1] for $\frac{d\Gamma}{dM^2}(\overline{B}^o \rightarrow D^{*+}\pi^+\pi^-\pi^-\pi^o)$ plotted as a function of the four-pion invariant mass squared, normalized to the semi-leptonic rate, and compared with the LLW prediction [2]. We also plot $\frac{d\Gamma}{dM^2}(\overline{B}^o \rightarrow D^{*o}\pi^+\pi^+\pi^-\pi^-)$, again normalized to the semileptonic rate.

In principle a non-zero rate in the $D^{*o}(4\pi)^o$ final state is indicative of an additional contribution to the $D^{*+}(4\pi)^-$ final state, beyond what is expected in factorization, and needs to be subtracted to make an accurate prediction.[†] In fact, the $D^{*o}(4\pi)^o$ rate is consistent with zero in the mass squared region covered by the LLW prediction.

6 Conclusions

In conclusion we have made the first measurement of $\mathcal{B}(\overline{B}^o \rightarrow D^{*o}\pi^+\pi^+\pi^-\pi^-) = (0.30 \pm 0.07 \pm 0.06)\%$. The reaction has a large component of $D^{*+} \rightarrow D^{*o}\pi^+$. The relative rate for

$$\frac{\Gamma(\overline{B}^o \rightarrow D^{*o}\pi^+\pi^+\pi^-\pi^-)}{\Gamma(\overline{B}^o \rightarrow D^{*+}\pi^+\pi^-\pi^-\pi^o)} = 0.17 \pm 0.04 \pm 0.02 \quad . \quad (6)$$

LLW have used the $\overline{B}^o \rightarrow D^{*+}\pi^+\pi^-\pi^-\pi^o$ reaction to test the 4π mass dependence of factorization that could point to the origin of factorization being perturbative QCD where

[†]If the $D^{*o}(4\pi)^o$ final state comes from D^{*+} production, then the relative contribution in the $D^{*+}(4\pi)^-$ final state is given by isotopic spin conservation to be one half.

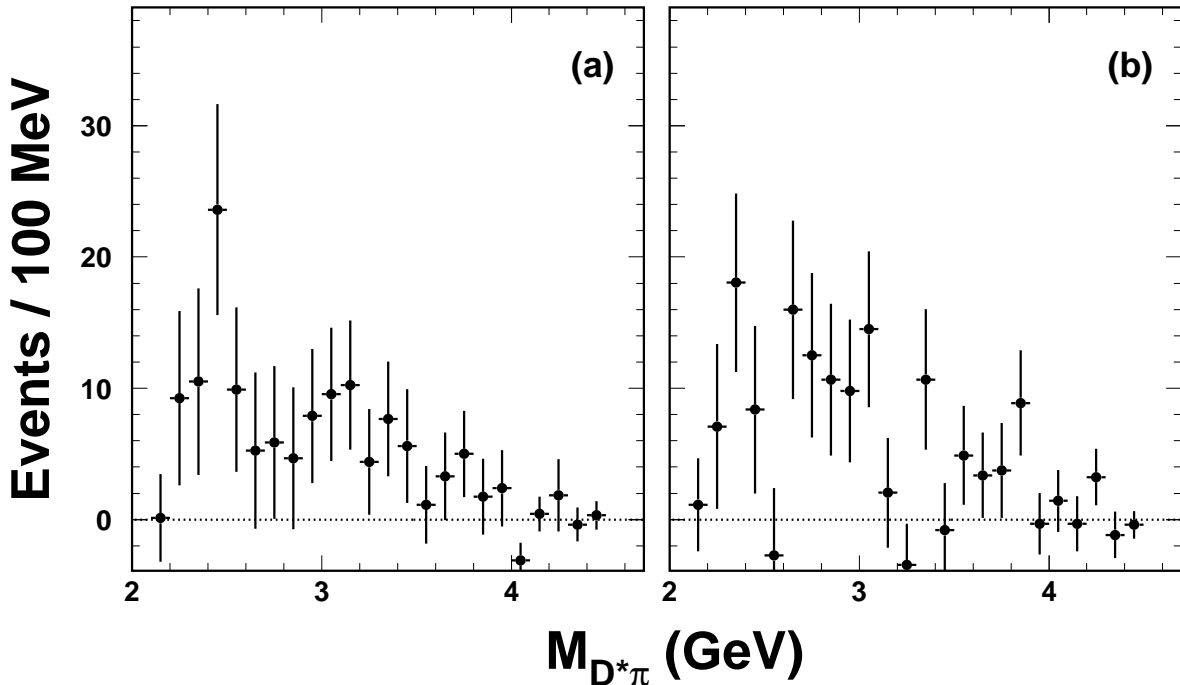


Figure 5: The invariant mass spectra of (a) $D^{*o}\pi^+$, and (b) $D^{*o}\pi^-$ for the final state $D^{*o}\pi^+\pi^+\pi^-\pi^-$, found by fitting the B yield in bins of 4π mass. (There are two combinations per event.)

the approximation should weaken with 4π mass or the large N_c limit, where N_c refers to the number of colors.

LLW suggested that the presence of D^{**} production might cause their factorization test to be inaccurate. We have found such a presence in the analogous reaction $\overline{B}^0 \rightarrow D^{*o}\pi^+\pi^+\pi^-\pi^-$. However, the 4π mass region that is populated is higher than that used by LLW so no effect on their prediction can be inferred.

7 Acknowledgements

We thank Z. Ligeti, M. Luke and M. Wise for interesting discussions.

References

- [1] J. P. Alexander *et al.* (CLEO), “First Observation of $\overline{B} \rightarrow D^{(*)}\rho'^-, \rho'^- \rightarrow \omega\pi^-$,” CLNS 01/1724, 2001 [hep-ex/0103021].
- [2] Z. Ligeti, M. Luke and M. B. Wise, “Comment on Studying the Corrections to Factorization in $B \rightarrow D^{(*)}X$,” LBNL-47551, UTPT-01-05, CALT-68-2316 (2001) [hep-ph/0103020].

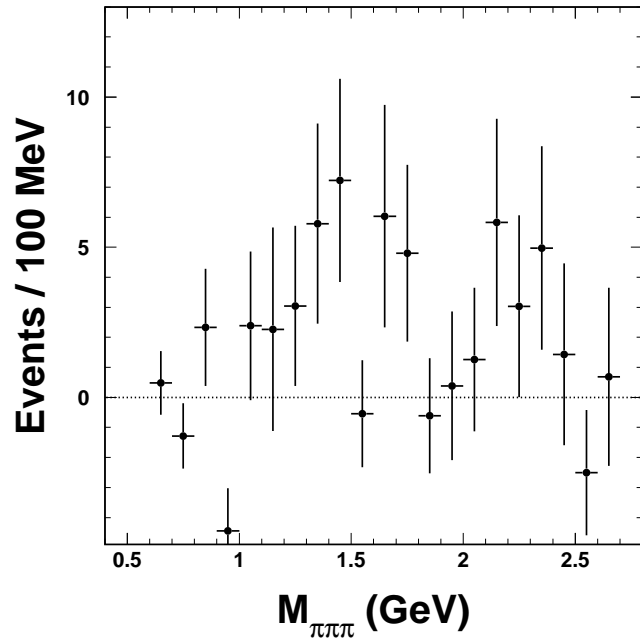


Figure 6: The invariant mass spectra of $\pi^+\pi^-\pi^-$ when the $D^{*0}\pi^+$ invariant mass is between 2.3 and 2.6 GeV.

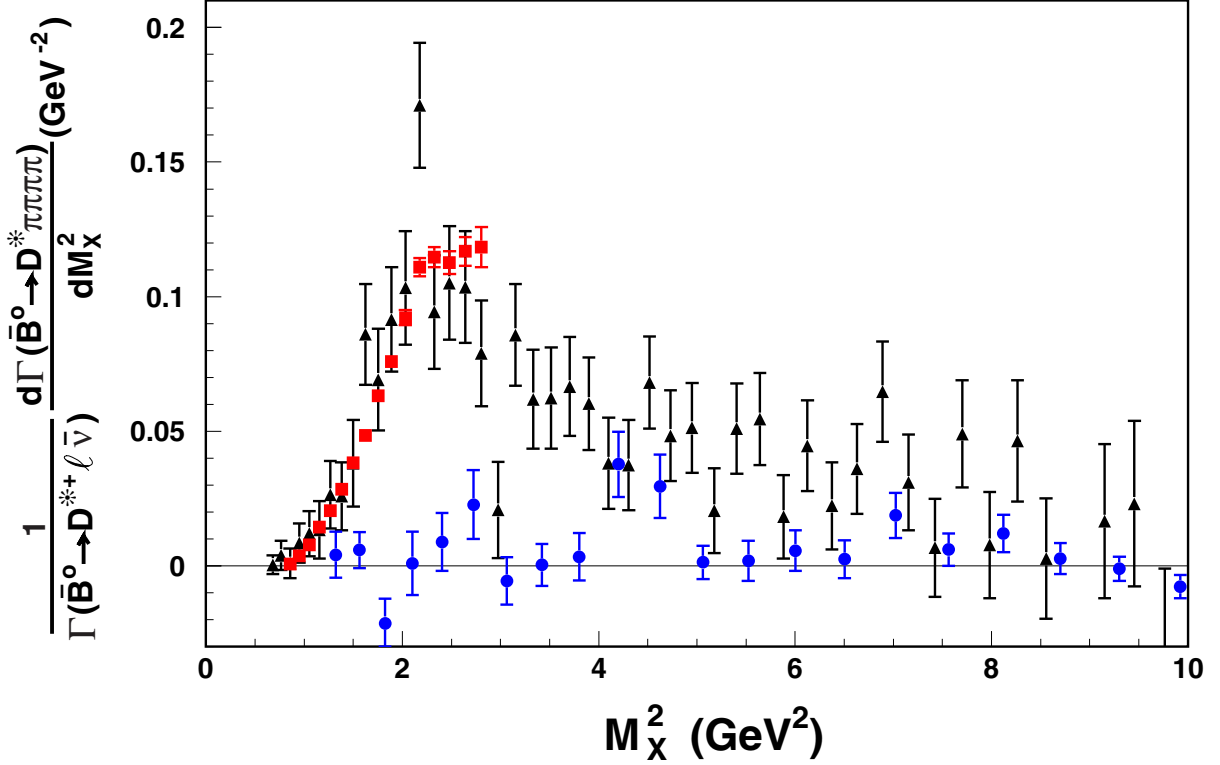


Figure 7: $\frac{d\Gamma}{dM_X^2}(\overline{B}^o \rightarrow D^* \pi \pi \pi \pi)$, where M_X^2 is the 4π invariant mass squared, normalized to the semileptonic width $\Gamma(\overline{B}^o \rightarrow D^* \ell^- \bar{\nu})$. The circles are the CLEO data for $\overline{B}^o \rightarrow D^{*0} \pi^+ \pi^+ \pi^- \pi^-$, the squares the model prediction of LLW and the triangles are the data for $\overline{B}^o \rightarrow D^{*+} \pi^+ \pi^- \pi^- \pi^0$. There is an additional systematic normalization uncertainty on the triangle points of 9% and on the circles of 16%.

- [3] K. Edwards *et al.* (CLEO), Phys. Rev. **D61** 072003 (2000).
- [4] J. Bjorken, Nucl. Phys. B (Proc. Suppl.) **11**, 325 (1989); D. Bortoletto and S. Stone, Phys. Rev. Lett. **65**, 2951 (1990); M. J. Dugan and B. Grinstein Phys. Lett. B **255**, 583 (1991) and references contained therein; T. E. Browder, K. Honscheid and S. Playfer, “A Review of Hadronic and Rare B Decays,” in B Decays (Revised 2nd Edition), ed. S. Stone, World Scientific, Singapore, 1994, p158 and references contained therein.
- [5] The CLEO II detector is described in Y. Kubota *et al.*, Nucl. Instrum. Methods A **320**, 66 (1992), and CLEO II.V in T. Hill, *ibid* A **418**, 32 (1998).
- [6] G. Fox and S. Wolfram, Phys. Rev. Lett. **23**, 1581 (1978).
- [7] D. Groom *et al.*, The European Physical Journal **C15**, 1 (2000).
- [8] We do not find significant differences between the CLEO II and II.V data sets.
- [9] M. S. Alam *et al.* (CLEO), Phys. Rev. **50**, 43 (1994); S. Anderson *et al.* (CLEO), “Observation of a Broad $L = 1$ cq state in $B^- \rightarrow D^{*+}\pi^-\pi^-$ at CLEO,” CONF 99-6 (1999).

8 Appendix A: Details of Selection Requirements

8.1 Charged Track Cuts

Tracks must pass trackman

$KINCD$ must be zero

For tracks above 250 MeV we require $|DBCD| < 0.005$ and $|Z0CD - ZVPTX| < 0.03$

For tracks below 250 MeV we require $|DBCD| < 0.01$ and $|Z0CD - ZVPTX| < 0.05$

8.2 Particle Identification Cuts

For tracks above 900 MeV/c we do not require any particle identification

For tracks below 900 MeV/c we require 3σ consistency, if the information is present ($IQUALDI > 0$)

8.3 Photon Selection

We use XBAL

We require that the bump energy be > 30 MeV in the good barrel region, $|\cos \theta| < 0.707$

The E9/E25 distribution must look like a photon, $E925U > C92501$

Photon candidates must not be shower fragments, $IBSTOP = 0$

Finally, the angle with closest charged track must be $> 20^\circ$.

8.4 π^0 Selection

If both bumps belong to a multi-bump region, they must come from the same region. We require that the diphoton invariant mass be between -3.0 to $+2.5\sigma$. The candidates are kinematically fit by restraining their invariant mass be equal to nominal π^0 mass.

8.5 D^0 Selection

We require that the $K^-\pi^+$ invariant mass within 2.5σ from known D^0 value. The D^0 width varies with the momentum p , $\sigma = p \times 0.93 \times 10^{-3} + 6.0$ (units of MeV).

8.6 D^{*0} Selection

For all $D^0\pi^0$ combinations, we calculate the difference of $D^0\pi^0$ invariant mass and D^0 reconstructed mass. Candidates with mass difference consistent with known value within 2.5σ are selected. The resolution σ is 0.90 MeV.

9 Appendix B: ΔE versus M_B Scatter plot

In Fig. 8 we show the correlation between the reconstructed B mass and the difference between the reconstructed energy and the beam energy. The solid rectangle indicates the signal region.

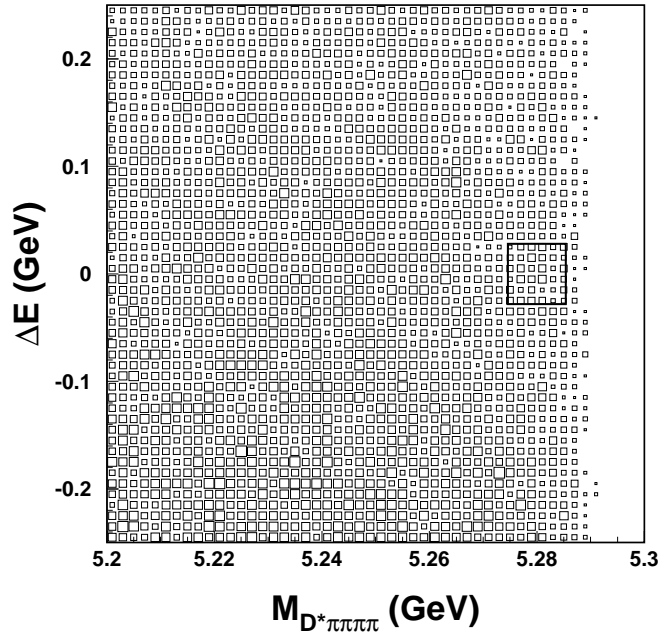


Figure 8: Plot of ΔE versus M_B .